

Received: 2017.04.04
Accepted: 2017.05.04
Published: 2017.05.22

Folic Acid-Targeted Etoposide Cubosomes for Theranostic Application of Cancer Cell Imaging and Therapy

Authors' Contribution:
Study Design A
Data Collection B
Statistical Analysis C
Data Interpretation D
Manuscript Preparation E
Literature Search F
Funds Collection G

ACE 1 **Yong Tian***
ABDG 1,2 **Jian-chun Li***
DE 3 **Jin-xiu Zhu**
CD 1 **Na Zhu**
EF 1 **Hong-min Zhang**
DG 1 **Lili Liang**
FG 2 **Lingyi Sun**

1 School of Pharmacy, Bengbu Medical College, Bengbu, Anhui, P.R. China
2 Molecular Imaging Lab, School of Medicine, University of Pittsburgh, Pittsburgh, PA, U.S.A.
3 The 1st Affiliated Hospital of Bengbu Medical College, Bengbu, Anhui, P.R. China

* These authors contributed equally to this work

Corresponding Author:

Jian-Chun Li, e-mail: lijc66577@sohu.com

Source of support:

This work was supported by Scientific Research Projects of Bengbu Medical College of Anhui Province (No. BYKY1609ZD); Scientific Research Innovation Projects of Bengbu Medical College of Anhui Province (No. Byycxz1623, No. Byycxz1556); and the Visiting Scholar Foundation of Anhui Province (No. gxfxZD2016148)

Background: The aim of this study was to develop a novel Poloxamer-based drug delivery system featuring a tumor-targeting folate moiety, which was expected to provide better targeting properties and therapeutic effects compared with the traditional cubosomes (Cubs).





Material/Methods: Both folate-modified Cubs containing etoposide (ETP-Cubs-FA) and normal cubic nanoparticles loaded with etoposide (ETP-Cubs) were prepared through the fragmentation of bulk gels under the homogenization condition of 1500 bar, and a mean particle size of around 180 nm was obtained with a narrow size distribution. The cubosomes were further characterized by *differential scanning calorimetry* (DSC) and *Polarized light microscopy* (PLM). The release of ETP *in vitro* from these nanoparticles was found to be 82.5% at 36 h, showing a sustained release property compared with the free drug administration.

Results: Folate-modified cubosomes exhibited best anti-proliferative activity followed by normal cubosomes and the free drug. A further cell uptake study of Rhodamine B-loaded Cubs-FA (Rh-B-Cubs-FA) showed a marked increase of cellular accumulation compared with free Rh-B and Rh-B-loaded Cubs (Rh-B-Cubs). *In vivo* Rh-B-based tumor imaging demonstrated that Cubs-FA specifically targeted the tumor tissue.

Conclusions: The folate-modified cubosomes containing ETP may be a promising drug candidate for antitumor treatment.

MeSH Keywords: **Drug Delivery Systems • Etoposide • Folate Receptor 1**

Full-text PDF: <http://www.medscimonit.com/abstract/index/idArt/904683>

 3421  2  9  43



Background

The concept of bi-continuous liquid crystal phase was first developed in the late 1960s, and its geometric construction was later fulfilled in the mid-1970s [1,2]. Among these phases, the most studied and interesting are probably the reverse bi-continuous cubic phases, especially those based on the monoolein-water system [3,4]. Accompanied with the fast development of modern pharmaceutical nanotechnology, their applications in different pharmaceutical fields such as enzymes, antitumor drugs, antibiotics, and analgesic delivery have been extensively investigated and reviewed [5]. The cubic liquid crystal, which could be dispersed in water, exhibited good biocompatibility and bioadhesivity [6,7]. With the promising properties mentioned above, these multifunctional delivery systems can be administered via different approaches, such as intravenous, oral, percutaneous, and ophthalmic injections [8–11].

ETP is a topoisomerase II inhibitor which exhibited anti-proliferative activity via causing DNA breaks [12–14]. However, its poor solubility limited its clinical application, and reported ETP delivery systems have often been associated with adverse effects [15]. In this proof of principle study, we used ETP as the model drug to explore the potential application of cubosomes in developing a novel drug delivery system for cancer treatment.

Although various emulsifiers have been investigated for preparing novel lipid-based dispersion systems from the cubic liquid crystal [16,17], the most widely used system is the ternary system of Glycerol monooleate (GMO) and P407-water, in which P407 is commonly applied in stabilizing the dispersion of CUBS, while the unique structure of GMO makes CUBS able to be embedded, controlling the release of drugs with different molecular weights and polarities [18–20].

The modern cancer treatment, targeting therapy, featuring selectively delivered anti-cancer agents to the tumor site while minimizing its accumulation at other normal organs, has been considered a promising strategy to reduce adverse effects during treatment [21]. Folate receptor, which is known to be vastly overexpressed on malignant cancer cells [22–24], has been proposed as a promising target for molecular imaging [25]. In this study, a straightforward one-step reaction to prepare the P407-FA adduct was carried out. Since surface functionalization of hexosomes and cubosomes with folate residues has been reported [26,27], we hypothesized that the decoration of the cubosomes surface with P407-FA can enhance its tumor-targeting property via the FA-mediated mechanism.

This study focused on developing a novel type of cubic liquid crystal decorated by P407-FA as a potential targeted ETP delivery system. Replacement of the stabilizer with mixtures of Poloxamer-407 and folate-conjugated P407 does not affect

the inner structure of cubosomes. The *in vitro* release of ETP from ETP-CUBS and ETP-CUBS-FA was investigated in this study. Physical properties of ETP-CUBS and ETP-CUBS-FA are characterized by ¹H-NMR, DSC and PLM. *In vitro* anti-proliferative activity of ETP-CUBS and ETP-CUBS-FA against human breast adenocarcinoma MCF-7 cells were evaluated by the MTT assay and further compared with the free ETP treatment. The cellular uptake of CUBS-FA was further investigated via Rh-B-loaded CUBS-FA. Additionally, the *in vivo* tumor-targeting property of Rh-B-loaded CUBS and CUBS-FA was studied using the Fluorescence Imaging System.

Material and Methods

Glycerol monooleate was purchased from Baoman Co. Ltd. (Shanghai, China). Poloxamer 407, folic acid, and 1, 1-Carbonyldiimidazole (CDI) were provided by Yuan Ye Co. Ltd. (Shanghai, China). Etoposide was purchased from Adamas Reagent Co., Ltd. A dialysis bag with a molecular weight cutoff of 14 000 Da (Viskase Companies, Inc., Darien, IL, USA) was used. The Milli-Q grade water was purified using a Millipore system throughout this study. All other reagents used in this study were high-performance liquid chromatography (HPLC) grade or analytical grade.

Cells

Human breast carcinoma cell lines (MCF-7) were kindly provided by the Institute of Pharmacy of Bengbu Medical college (Anhui, China) and cultured in folate-free DMEM medium supplemented with 10% FBS. All cells were cultured in a 37°C incubator with 5% CO₂.

Analytical system

The analysis was performed on reverse-phase high-performance liquid chromatography (HPLC) (Ultimate 3000, American) via an isocratic elution with a mobile phase consisting of 30% acetonitrile and 70% pH=4.0 acetate buffer. The flow rate of the mobile phase was 1 mL/min with an injection volume of 20 µL, and the wavelength was set at 254 nm. The separation of samples was achieved by HPLC using packed column 250×4.6 mm with particle size of 5µm (Kromasil C18; Biomics™ Co. Ltd., Nantong, China).

Synthesis and characterization of FA-conjugated P407

P407-FA was synthesized via a previously reported method with modifications [28]. Firstly, 87.58 mg (0.20 mmol) of FA was dissolved in 5 ml dried DMSO and added to a one-neck flask. Then, 35.32 mg (0.22 mmol) of CDI was added to the solution, and the reaction was stirred for 24 h at room temperature in

the dark, then we added 0.62 g (0.05 mmol) of P407 which had been previously dried overnight in a vacuum and the reaction was allowed to proceed in the dark for 1 day at room temperature. After the reaction was completed, the mixture was dialyzed for 5 d in a dialysis bag with a molecular cut off of 3000 to remove free FA. P407-FA was recovered via lyophilization. The resulting product was dried in a vacuum oven for 2 d and stored in a dry box, yielding 56% w/w of product.

Prepared P407-FA was characterized by ¹H-NMR and differential scanning calorimetry (DSC-60; Shimadzu Corporation, Kyoto, Japan). ¹H-NMR spectrum of P407-FA was recorded on a Gemini-200 spectrometer (Varian, CA, USA) using DMSO-d₆ as the solvent. UV-Vis spectra were acquired using a UV-1601 spectrophotometer (Shimadzu Corp., Kyoto, Japan) to determine the degree of conjugation of FA by measuring the absorbance at 360 nm.

Sample preparation

The drug-loaded nanoparticles system was prepared and stabilized by dispersing the appropriate amount of GMO in water solutions with different P407/P407-FA mixtures (100: 0, 80: 20 wt%/wt%) using a high-pressure homogenizer (JN-02HC; JUNENG Co. Ltd., Guangzhou, China) (9 cycle, 1500 bar pressure) [29]. ETP-Cubs and ETP-Cubs-FA were obtained by dispersing ETP acetone solution in melted lipids and subsequently removing acetone via continuous stirring in a 60°C water bath. The sample volume was usually 10 ml consisting of approximately 96.8 wt% water, 2.9 wt% GMO, and 0.3 wt% Pluronic mixture. Rhodamine B and ETP quantities were 4.8×10⁻⁴ and 1.5×10⁻³ wt%, respectively.

Characterization of cubosomes

Particles size and zeta potential

The particle size, size distribution, and zeta potential of prepared cubosomes were measured by photon correlation spectroscopy using a NanoZS90 zeta sizer (Malvern Instruments, Malvern, UK), which is based on the principles of Brownian motion. Samples were diluted with deionized water with a dilution factor of 1: 50. Samples were sonicated for 5 min before measurement. The results presented here are the average of 3 successive circulation measurements.

Encapsulation efficiency

The entrapment efficiency (EE%) of prepared cubosomes was determined by dialysis as follows [30]: 1 ml dispersion of cubosomes was loaded into a dialysis bag (MWCO 14000 Da, USA), which was subsequently stirred in a flask filled with 50 ml water for 4 h. ETP was determined by measuring the concentration of drug inside or outside the dialysis bag via HPLC.

The entrapped efficiency was calculated by the following equation:

$$EE\% = (C_{total} - C_{free}) / C_{total} \times 100\%$$

C_{total} represents the total concentration of drug in the cubosomes;

C_{free} represents the concentration of free drug in the dialysis fluid.

Polarized light microscope (PLM)

The polarization phenomenon was investigated using PLM. The observation was recorded, and the drawing of the sample was conducted at room temperature [31].

Differential scanning calorimetry (DSC)

To characterize thermodynamic properties of different materials, including GMO, P407, ETP, physical mixtures, ETP-Cubs, and ETP-Cubs-FA, approximately 5–10 mg sample was sealed in the aluminum crimp cell and heated to 350°C at an increasing rate of 10°C/min from 35°C in a nitrogen atmosphere (VP-DSC, Microcal, USA). Results were recorded and then analyzed using OriginPro 8.0.

In vitro drug release from cubosomes

The *in vitro* release of ETP from cubic nanoparticles was investigated using the dynamic dialysis bag method [32]. The dialyzed suspension containing ETP-Cubs-FA or the aqueous solution of the plain drug (containing 20% acetonitrile) was placed in a dialysis bag (MWCO 14000 Da, Viskase Companies, Inc., Darien, IL, USA) and then immersed in the release media (phosphate-buffered saline with 10% ethanol) that was thermostatically maintained at 37±0.5°C and stirred at 100 rpm. We withdrew 100 µL of sample at different time intervals, and volumes lost by the withdrawal of samples were replaced with fresh medium. The concentration of released ETP was then measured by the HPLC method.

Cytotoxicity assay

The antitumor activity of the drug-loaded cubosomes was evaluated by the MTT method [33]. Human breast carcinoma MCF-7 cells were cultured in the growth medium DMEM supplement with 10% fetal bovine serum (FBS), 100U/mL penicillin, and 100 µg/mL streptomycin. The cells were seeded at a density of 10 000 cells/well on 96-well plates and allowed to grow overnight for reattachment. The growth medium was then replaced with 200 µL medium containing increasing concentrations of each of the following substances: free ETP dissolved in DMSO, ETP-Cubs, and ETP-Cubs-FA. The cells were incubated

for 24 h and then washed 3 times with PBS. Subsequently, the MTT solution was added to each well and the cells were incubated for an additional 4 h at 37°C. Thereafter, the medium was removed and DMSO (200 µl) was added to each well. Absorbance at 490 nm was recorded.

Cell uptake test

For qualitative analysis of the cellular uptake in this study, the internalized nanoparticles in MCF-7 cells were measured [34]. Rh-B-Cubs-FA were prepared in the same way as preparing ETP-Cubs-FA. Different formulations of Rh-B: 50 µg/mL of free Rh-B, Rh-B-loaded Cubs, and Rh-B loaded Cubs-FA were evaluated on separate MCF-7 cells. MCF-7 cells were seeded in 6-well plates at a density of approximately 400 000 per well and incubated using DMEM medium for 24 h. Rh-B-Cubs-FA, Rh-B-Cubs, and Rh-B solutions were then added into different wells, and cells were further incubated at 37°C for 4 h. After that, cells were fixed with 4% formaldehyde for about 10 min, and the cell nuclei were stained with 4,6-diamidino-2-phenylindole (DAPI) for 3 min. Then, the fluorescent images of different samples were obtained using a Nikon Eclipse E400 microscope.

Targeted imaging

A breast carcinoma mouse model was established by subcutaneous inoculation of 5×10^6 MCF-7 cells in 0.1 ml of PBS (pH 7.4) into nude female BALB/c mice. Tumor-targeted imaging was carried out when the tumor grew to approximately 0.4 cm³.

The tumor-targeted imaging of MCF-7 breast cancer-bearing mice was conducted using a Small Animal *In Vivo* Fluorescence Imaging System (Bruker Corporation, Billerica, MA, USA). Briefly, the Rh-B-Cubs and Rh-B-Cubs-FA solutions were injected into separate tumor-bearing groups of mice through the tail vein at an equivalent concentration (2 mg Rh-B/kg per mouse). Fluorescence images at an excitation wavelength of 530 nm and an emission wavelength of 600 nm were recorded at 2, 6, 8, 12, and 24 h post-injection.

Results

Synthesis and characterization of FA-conjugated P407

The DSC curves of FA (A), physical mixture (B), and P407-FA (C) are shown in Figure 1. The thermogram of FA showed 1 endothermic peak at 120°C. The physical mixture showed 2 different peaks corresponding to P407 and FA, the first peak was at 60°C and the second at 120°C. In DSC of the P407-FA, characteristic peaks of the FA had disappeared, indicating the P407-FA was pure, not a mixture of P407 and FA. The ¹H-NMR

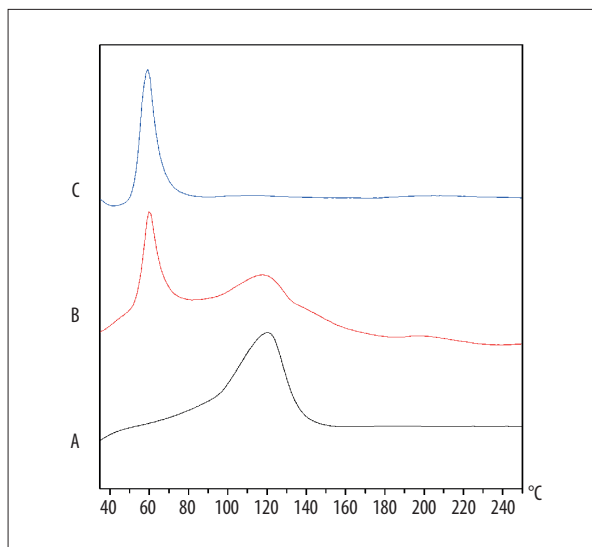


Figure 1. The DSC thermograms of folate (A), the mixture of folate and P407 (B), P407-FA (C).

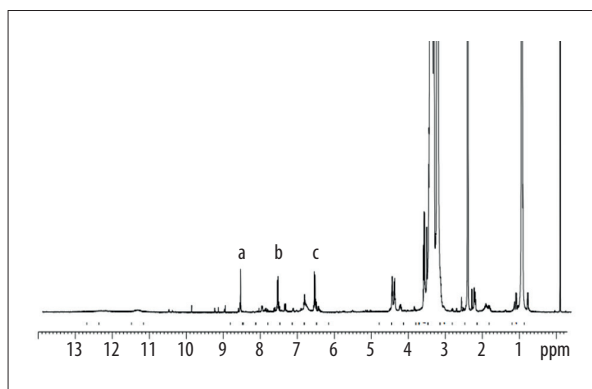


Figure 2. ¹H-NMR spectrum of P407-FA. Peaks a-c represent aromatic protons in FA.

spectrum of P407-FA in DMSO-d₆ is shown in Figure 2. FA signals appeared at 6.6 ppm (3,5-H of benzene in folate), 7.6 ppm (2,6-H of benzene in folate), and 8.6 ppm (C7-H of pteridine in folate) [35]. The conjugation extent of folic acid (wt%) in P407-FA was measured by a UV-Vis spectrum, and the result was 5.4 wt%.

Sample preparation and characterization of cubosomes

Taking into account both the preparation efficiency and the rapid dispersion of the drug, the precursor method was chosen [36]. To increase the solubility of the ETP in the melted lipids, ETP was dissolved in the acetone solution, followed by the removal of acetone in a 60°C water bath. The entrapment efficiency for the Cubs and Cubs-FA were approximate 87.3% and 84.7%, respectively.

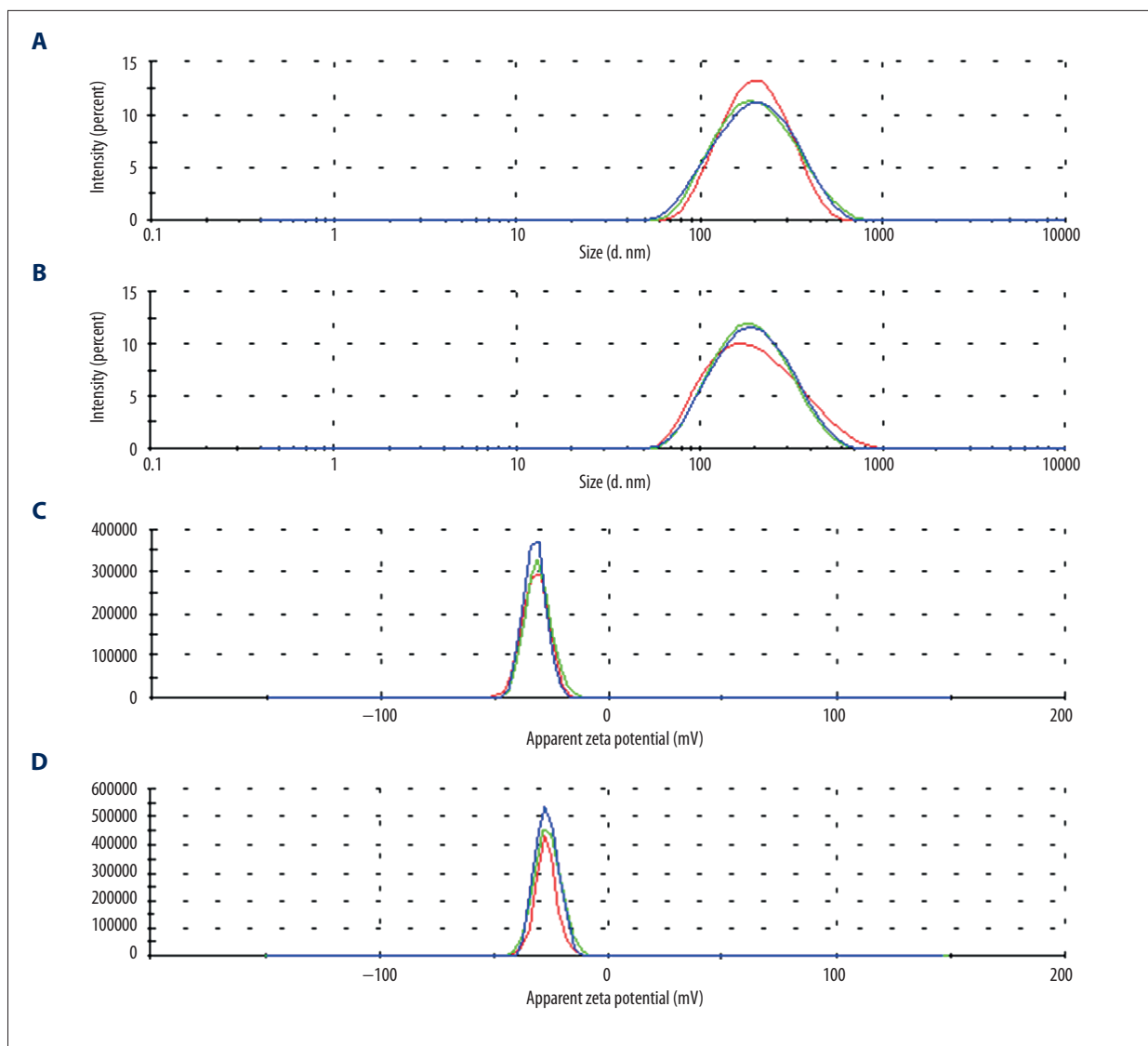


Figure 3. Size and Zeta distribution of cubosomes. Different colors represent 3 tests (n=3). (A) Size distribution of ETP-Cubs; (B) Size distribution of ETP-Cubs-FA; (C) Zeta distribution of ETP-Cubs; (D) Zeta distribution of ETP-Cubs-FA.

Table 1. Effects of ETP-Cubs and ETP-Cubs-FA on particles size, zeta potential and PDI of the cubosomes (n=3).

Sample	Average size (nm)	Zeta potential (mv)	PDI
ETP-Cubs	173.6±1.6	-31.9±0.8	0.174±0.019
ETP-Cubs-FA	180.9±1.4	-26.7±0.3	0.167±0.007

Particles size and zeta potential

Figure 3 shows the size distribution and the zeta potential of the ETP-Cubs and ETP-Cubs-FA. The average diameter of cubosomes was smaller than 200 nm without any greater than 1 μm, indicating a unimodal pattern. Table 1 shows that the zeta potential of ETP-Cubs was a little higher than that of the ETP-Cubs-FA. We also found that the average diameter of the

particles increased from 173.6±1.6 nm to 180.9±1.4 nm when the cubosomes were modified by folate.

Polarized light microscopy (PLM)

The optical birefringence phenomenon of cubosomes was also studied. Due to the optically isotropic characteristic, the picture of the polarity of cubosomes showed the dark field. We also made a

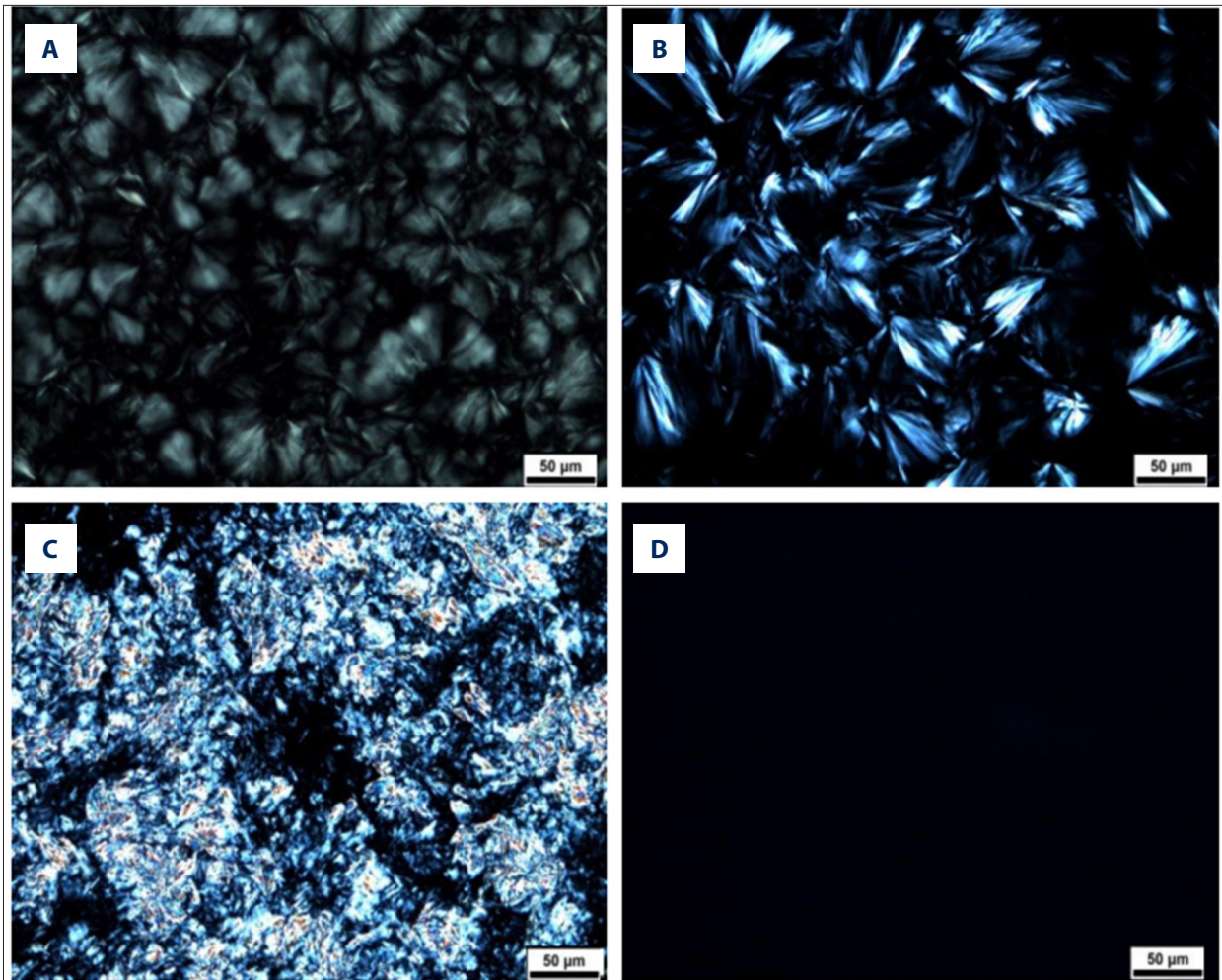


Figure 4. Different states of liquid crystal. (A) and (B) Represent lamellar liquid crystal; (C) No liquid crystal; (D) Cubic liquid crystal.

different prescription in this study, as can be seen from Figure 4 A (GMO: P407, 5: 5), B (GMO: P407, 4: 6) representing lamellar crystal, C (GMO: P407, 2: 8) representing none-liquid crystal, and D (GMO: P407, 9: 1) showing an isotropic arrangement with a dark sight field, indicating that the sample is cubic in morphology.

Differential scanning calorimetry (DSC)

Differential scanning calorimetry is a rapid and reliable method to screen different materials. The DSC curves of GMO (A), P407 (B), ETP (C), their mixture (D), the preparation of the ETP-Cubs (E, prepared with 100% P407), and the preparation of the ETP-Cubs-FA (F, prepared with 100% P407-FA) are shown in Figure 5 and the DSC curves of FA are shown in Figure 1. The thermogram of ETP and P407 shows their endothermic peaks at 265°C and 60°C, respectively. Unlike GMO with no clear endothermic peak, the physical mixture showed several characteristic peaks corresponding to ETP and P407. DSC of ETP-Cubs and ETP-Cubs-FA showed that characteristic peaks of the drug and P407 had disappeared, indicating the formation of a cubic

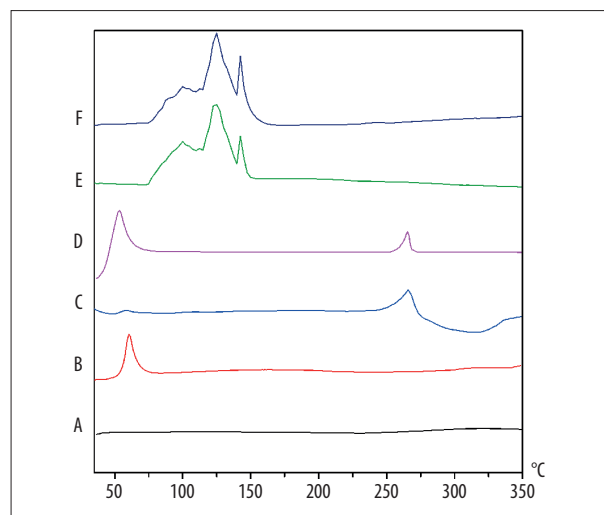


Figure 5. The DSC thermograms of GMO (A), P407 (B), ETP (C), Their mixture (D), ETP-Cubs (E, prepared with 100% P407), and ETP-Cubs-FA (F, prepared with 100% P407-FA).

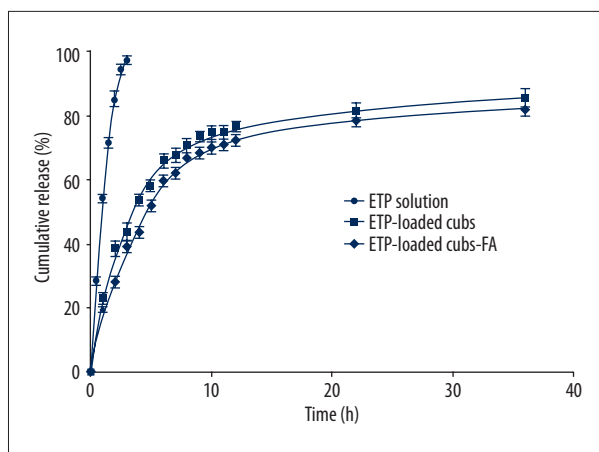


Figure 6. Release profile of ETP from ETP solution (●); ETP-Cubs (■); ETP-Cubs-FA (◆).

liquid crystal. In addition, cubic crystal gradually transformed into a hexagonal liquid crystal when the temperature exceeded 60°C and further transformed into a lamellar liquid crystal when the temperature exceeded 120°C. After 130°C, the liquid crystal structure was completely destroyed [37].

In vitro drug release from cubosomes

The *in vitro* release of ETP from the cubosomes was evaluated in phosphate-buffered saline (containing 20% ethanol). Ethanol was used to enhance the solubility of ETP in the release media

so that a sink condition could be created. The cumulative release of ETP from Cubs or Cubs-FA was performed, and the ETP solution was used as a control. As shown in Figure 6, ETP-loaded Cubs and ETP-loaded Cubs-FA exhibited similar release patterns. The cumulative release percentages of ETP from ETP-Cubs and ETP-Cubs-FA within 36 h were 85.6% and 82.5%, respectively. The cumulative release of free ETP was rapid and reached 100% almost in the first 2 h. The results indicated that the ETP-loaded Cubs and ETP-loaded Cubs-FA possessed a sustained ETP release efficacy compared with ETP solution.

In vitro cytotoxicity assay

To evaluate the toxicity of blank Cubs and Cubs-FA, MCF-7 cells were incubated with blank cubosomes for 24 h at concentrations ranging from 10 to 1000 µg/ml (GMO concentration), the nanoparticle formulations at a concentration of 1: 10 (100 µL/mL of medium). As shown in Figure 7A, the cell viability, as determined by the MTT assay, indicates that both Cubs and Cubs-FA are non-toxic to the MCF-7 cells.

The anti-proliferative activity of ETP in different formulations was evaluated by the MTT assay using the human breast carcinoma cell line MCF-7, which expresses high levels of folate receptors [34,38]. In Figure 7B, ETP-Cubs demonstrated a significantly superior cytotoxicity compared with free drug. IC₅₀ values of the 3 groups increased in order of ETP>ETP-Cubs>ETP-Cubs-FA in MCF-7 cell lines (Table 2). This phenomenon suggests

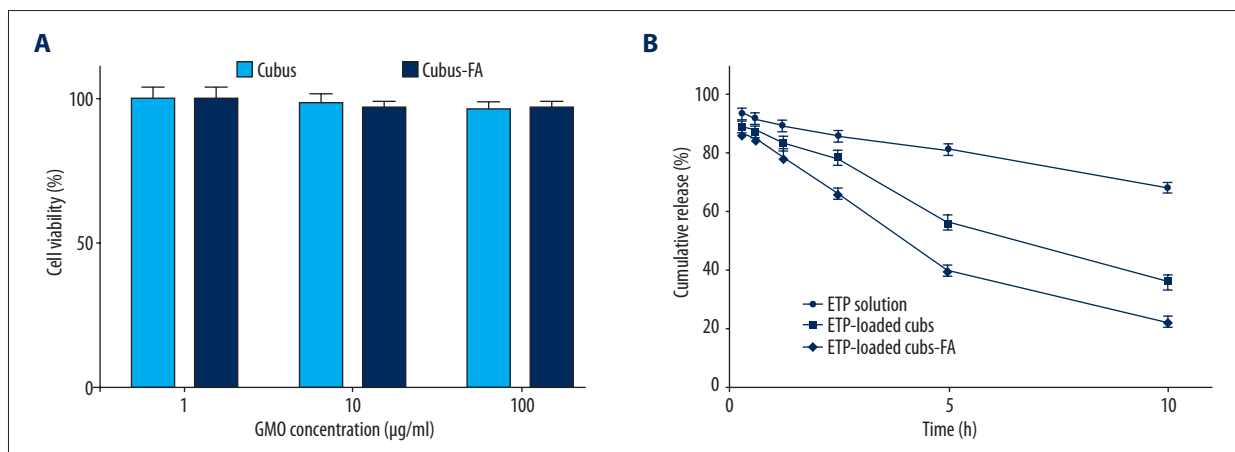


Figure 7. Cell viability of blank cubosomes and cytotoxicity of ETP and ETP-Cubs -FA. (A) Cell viability of MCF-7 cells after 24-h treatment with Cubs or Cubs-FA was determined by MTT. (B) *In vitro* cytotoxicity assessment of free ETP, ETP-Cubs, and ETP-Cubs-FA against MCF-7 cell lines.

Table 2. IC₅₀ values of ETP in free or cubosomes.

Cells	ETP (µg/ml)	ETP-Cubs (µg/ml)	ETP-Cubs-FA (µg/ml)
MCF-7	47.89±12.60	6.73±1.69*	3.60±0.68**

* p<0.05 vs. ETP, # p<0.05 vs. ETP-Cubs.

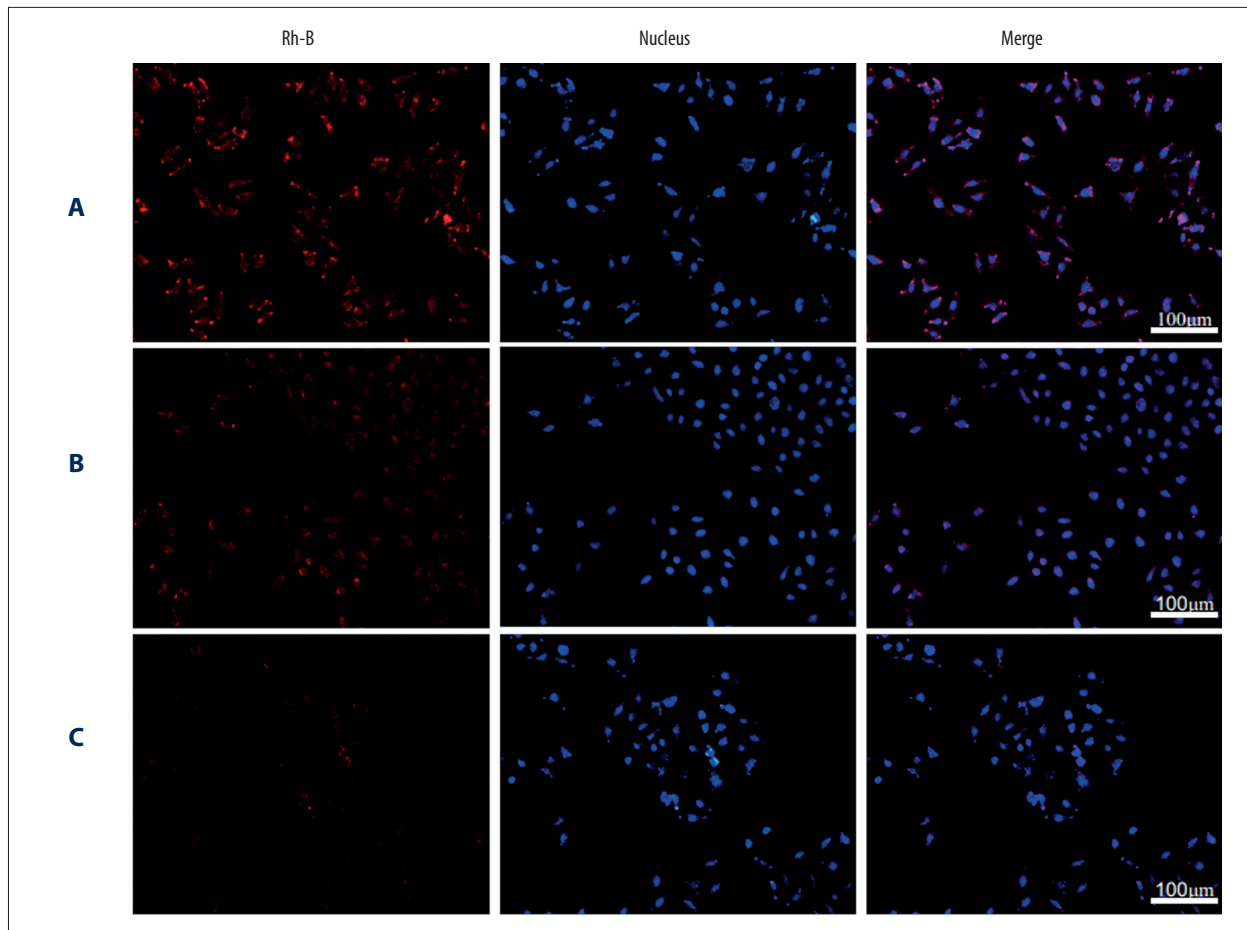


Figure 8. Rh-B uptake. Uptake of (A) Rh-B; (B) Rh-B-Cubs and (C) Rh-B-Cubs-FA at 4 h in MCF-7 cell lines.

that folate-modified ETP-Cubs might be transferred into MCF-7 cells more easily than the non-modified ETP-Cubs due to the interaction between the folate decorated on the Cubs surface and the folate receptors expressed on the MCF-7 cell surface. To test this hypothesis, cell uptake testing was carried out.

Cell uptake test

Rh-B is a substrate of P-gp and can be used as a marker for monitoring P-gp activity in cells [39]. Compared with free Rh-B, the accumulation of Rh-B in MCF-7 cells was increased by using Rh-B-Cubs and Rh-B-Cubs-FA (Figure 8). This observation indicates that the uptake of Rh-B was reversed by the P-gp efflux pump. Another explanation for this phenomenon is that Rh-B-Cubs inhibits the P-gp efflux pump by Pluronic [40]. The inner structure of cubosomes can be retained, which can be effectively stabilized by mixtures of P407 and P407-FA. This might be associated with the participation of P407 in the preparation of the cubic crystal.

More interestingly, the Rh-B-Cubs-FA demonstrated a marked increase of intracellular accumulation compared with

non-modified Rh-B-Cubs, which evidently was because of the active and effective process of the receptor-mediated endocytosis as well as the recycling of folate receptors after the internalization of folate-modified cubosomes [41].

Targeted imaging

In this study, we applied the fluorescent imaging technology to evaluate the *in vivo* tumor-targeting property of the nanoparticles using mice bearing the MCF-7 xenograft. As shown in Figure 9, Rh-B-Cubs and Rh-B-Cubs-FA exhibited different tumor-targeting efficiency during the monitoring period from 2 h to 24 h. At 2 h post-injection, the tumor fluorescence intensity in mice injected with the Rh-B-Cubs-FA was found to be higher than that in mice injected with Rh-B-Cubs. Between 6 h and 24 h post-injection, the tumor fluorescence intensity in mice treated with Rh-B-Cubs-FA increased more significantly as compared with that in mice treated with Rh-B-Cubs.

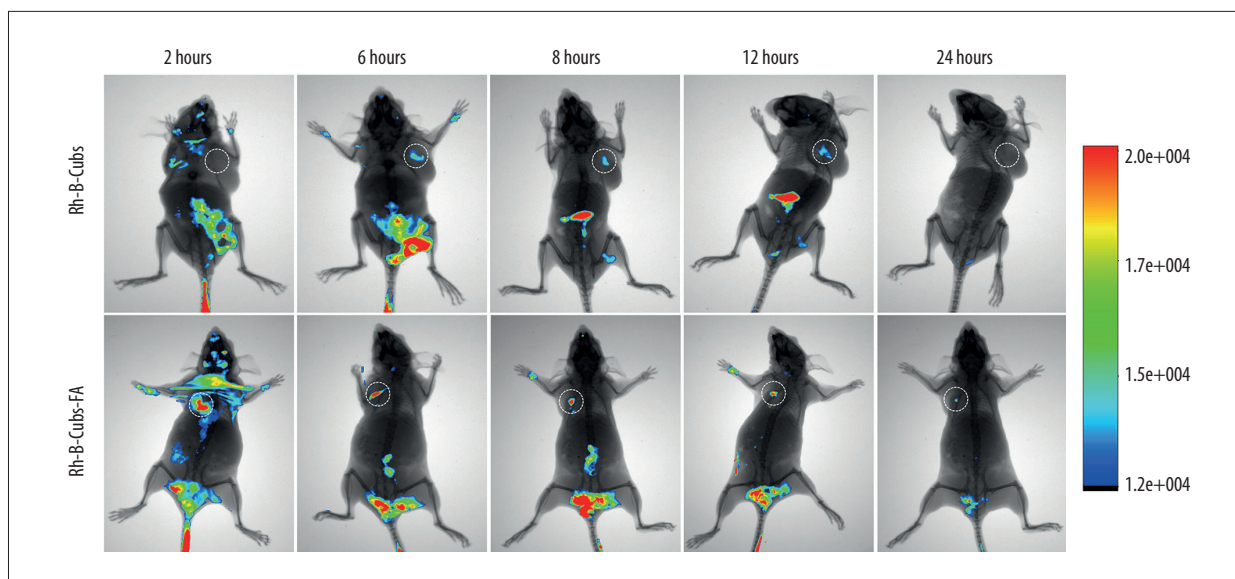


Figure 9. Whole-body and tumor fluorescence images (white circles indicate the inoculated tumor) in MCF-7 tumor-bearing mice after intravenous injection of Rh-B-Cubs and Rh-B-Cubs-FA.

Discussion

Lipid-based cubic liquid crystalline nanoparticles have recently captured the obvious interest of pharmaceutical research to enhance the bioavailability of lipophilic drugs [8]. Most of the research on cubosomes was on the cell level, and few *in vivo* studies have used intravenous administration [27,29]. Thus, it is necessary to estimate the influence of cubosomes *in vivo*, which to some extent plays a positive role in the drug delivery.

In our study, the tumor-targeting property of the Rh-B-Cubs was mainly due to their EPR effects, whereas the Rh-B-Cubs-FA can actively target the tumor via the interaction between the folate and the folate receptor overexpressed on the surface of MCF-7 breast cancer cells, leading to the high specific tumor uptake.

There have been several reports that the particles based on GMO and P407 are unstable in plasma [42]. P407, which provides steric stabilization to the particles, obviously cannot protect the cubic structure from environmental influences in plasma. In a previous study [43], the Cryo-TEM images of cubic dispersion based on GMO/P407 and human plasma after 24 h incubation at 37°C was investigated, revealing a broad diversity of structural change. Upon plasma contact, the phase transitions could be detected most clearly in an intermediate state, with hexagonal shape and showing smaller structure, sometimes retaining the cubic inner structure. The interaction between cubosomes and plasma results in alterations of particle structure, which might affect the liberation of incorporated drug substances.

However, in our study, at 2 h post-injection, there was tumor fluorescence intensity in mice injected with the Rh-B-Cubs-FA, and the cubosomes were not completely degraded at this time. Bye [11] reported that hexosomes are considerably less toxic and hemolytic to cells than are cubosomes. These cubosomes may occur in the phase transitions with smaller structure in the remaining cubic inner structure and hexagonal-phase nanoparticles (hexosomes) when the cubic liquid crystal nanoparticles pass through the blood system. In the first few hours, the folate-modified cubosomes target the tumor tissue through the folate receptors on the surface of tumor cells. However, the particles gradually undergo phase transformation, degradation, and the drug is released from the particles when the cubosomes was exposed to the blood for a long time. Although some *in vitro* studies have shown that cubosomes are unstable in plasma, the folate-modified cubosomes can target tumor tissue through the blood circulation.

Conclusions

In this study, the block copolymer P407 and its folate-modified version were successfully used in an 80/20(wt%) mixture to stabilize the cubic liquid crystal dispersion. The structure of the developed nanoparticles was confirmed by PLM and DSC, together with other cubosomes prepared via the traditional approach. ETP-Cubs and ETP-Cubs-FA demonstrated a more sustained release efficacy compared with ETP solution.

Moreover, an increasing tumor uptake of folate-conjugated Rh-B-Cubs compared to Rh-B-Cubs was observed both *in vitro* and *in vivo* using human breast cancer cells MCF-7, explaining the

superior cytotoxicity in the folate-modified ETP-loaded Cubs compared with free ETP and non-modified ETP-Cubs. These results suggest that the folate-modified cubosomes could be used as an efficient drug carrier for targeted delivery.

References:

- Luzzati V, Tardieu A, Gulik-Krzywicki T et al: Structure of the cubic phases of lipid-water systems. *Nature*, 1968; 220(5166): 485-88
- Scriven LE: Equilibrium bicontinuous structure. *Nature*, 1976; 263: 123-25
- Larsson K: Two cubic phases in monoolein-water system. *Nature*, 1983; 304: 664
- Larsson K: Cubic lipid-water phases: Structure and biomembrane aspects. *J Phys Chem*, 1989; 93: 73047314
- Barauskas J, Johnsson M, Tiberg F: Self-assembled lipid superstructures: Beyond vesicles and liposomes. *Nano Lett*, 2005; 5(8): 1615-19
- Larsson K: Aqueous dispersion of cubic lipid-water phases. *Curr Opin Colloid Interface Sci*, 2000; 5: 64-69
- Landh T, Larsson K: Particles, method of preparing said particles and uses thereof. US patent no. 5531925 (1996)
- Elnaggar YS, Etman SM, Abdelmonsif DA, Abdallah OY: Novel piperine-loaded Tween-integrated monoolein cubosomes as brain-targeted oral nano-medicine in Alzheimer's disease: Pharmaceutical, biological, and toxicological studies. *Int J Nanomedicine*, 2015; 10: 5459-73
- Hartnett TE, O'Connor AJ, Ladewig K: Cubosomes and other potential ocular drug delivery vehicles for macromolecular therapeutics. *Exp Opin Drug Deliv*, 2015; 12(9): 1513-26
- Peng X, Zhou Y, Han K et al: Characterization of cubosomes as a targeted and sustained transdermal delivery system for capsaicin. *Drug Des Devel Ther*, 2015; 9: 4209-18
- Bye N, Hutt OE, Hinton TM et al: Nitroxide-loaded hexosomes provide MRI contrast *in vivo*. *Langmuir*, 2014; 30: 8898-906
- Maswadeh HM, Aljarbou AN, Alorainy MS et al: Etoposide incorporated into camel milk phospholipids liposomes shows increased activity against fibrosarcoma in a mouse model. *Biomed Res Int*, 2015; 2015: 743051
- Park MJ: Prolonged response of meningeal carcinomatosis from non-small cell lung cancer to salvage intrathecal etoposide subsequent to failure of first-line methotrexate: A case report and literature review. *Am J Case Rep*, 2015; 16: 224-27
- Park MJ: Durable response of leptomeningeal metastasis of breast cancer to salvage intrathecal etoposide after methotrexate: A case report and literature review. *Am J Case Rep*, 2015; 16: 524-27
- Parmar JJ, Singh DJ, Lohade AA et al: Inhalational system for Etoposide liposomes: Formulation development and *in vitro* deposition. *Indian J Pharm Sci*, 2011; 73(6): 656-62
- Chong JY, Mulet X, Postma A et al: Novel RAFT amphiphilic brush copolymer steric stabilisers for cubosomes: Poly(octadecyl acrylate)-block-poly(polyethylene glycol methyl ether acrylate). *Soft Matter*, 2014; 10(35): 6666-76
- Azhari H, Strauss M, Hook S et al: Stabilising cubosomes with Tween 80 as a step towards targeting lipid nanocarriers to the blood-brain barrier. *Eur J Pharma Biopharm*, 2016; 104: 148-55
- Mohyeldin SM, Mehanna MM, Elgindy NA: Superiority of liquid crystalline cubic nanocarriers as hormonal transdermal vehicle: Comparative human skin permeation-supported evidence. *Exp Opin Drug Deliv*, 2016; 13(8): 1049-64
- Elgindy NA, Mehanna MM, Mohyeldin SM: Self-assembled nano-architecture liquid crystalline particles as a promising carrier for progesterone transdermal delivery. *Int J Pharm*, 2016; 501(1-2): 167-79
- Shi X, Peng T, Huang Y et al: Comparative studies on glycerol monooleate and phytantriol-based cubosomes containing oridonin *in vitro* and *in vivo*. *Pharm Dev Technol*, 2017; 22(3): 322-29
- Miller MJ, Foy KC, Kaumaya PT: Cancer immunotherapy: Present status, future perspective, and a new paradigm of peptide immunotherapeutics. *Discov Med*, 2013; 15(82): 166-76
- Qiao J, Dong P, Mu X et al: Folic acid-conjugated fluorescent polymer for up-regulation folate receptor expression study via targeted imaging of tumor cells. *Biosens Bioelectron*, 2016; 78: 147-53
- Bwatanglang IB, Mohammad F, Yusof NA et al: *In vivo* tumor targeting and anti-tumor effects of 5-fluorouracil loaded, folic acid targeted quantum dot system. *J Colloid Interface Sci*, 2016; 480: 146-58
- Liu J, Zhao D, He W et al: Nanoassemblies from amphiphilic cytarabine prodrug for leukemia targeted therapy. *J Colloid Interface Sci*, 2017; 487: 239-49
- Sega EI, Low PS: Tumor detection using folate receptor-targeted imaging agents. *Cancer Metastasis Rev*, 2008; 27: 655-64
- Aleandri S, Bandera D, Mezzenga R, Landau EM: Biotinylated cubosomes: A versatile tool for active targeting and codelivery of paclitaxel and a fluorescein-based lipid dye. *Langmuir*, 2015; 31(46): 12770-76
- Caltagirone C, Falchi AM, Lampis S et al: Cancer-cell-targeted theranostic cubosomes. *Langmuir*, 2014; 30(21): 6228-36
- Butt AM, Mohd Amin MC, Katas H: Synergistic effect of pH-responsive folate-functionalized poloxamer 407-TPGS-mixed micelles on targeted delivery of anticancer drugs. *Int J Nanomedicine*, 2015; 10: 1321-34
- Meli V, Caltagirone C, Falchi AM et al: Docetaxel-loaded fluorescent liquid-crystalline nanoparticles for cancer theranostics. *Langmuir*, 2015; 31(35): 9566-75
- Murgia S, Falchi AM, Meli V et al: Cubosome formulations stabilized by a dansyl-conjugated block copolymer for possible nanomedicine applications. *Colloids Surf B Biointerfaces*, 2015; 129: 87-94
- Li JC, Zhu N, Zhu JX et al: Self-assembled cubic liquid crystalline nanoparticles for transdermal delivery of Paeonol. *Med Sci Monit*, 2015; 21: 3298-310
- Jin X, Zhang ZH, Sun E et al: Enhanced oral absorption of 20(S)-protopanaxadiol by self-assembled liquid crystalline nanoparticles containing piperine: *In vitro* and *in vivo* studies. *Int J Nanomedicine*, 2013; 8: 641-52
- Rosa A, Murgia S, Putzu D et al: Monoolein-based cubosomes affect lipid profile in HeLa cells. *Chem Phys Lipids*, 2015; 191: 96-105
- Shen Z, Wu H, Yang S et al: A novel Trojan-horse targeting strategy to reduce the non-specific uptake of nanocarriers by non-cancerous cells. *Biomaterials*, 2015; 70: 1-11
- Wan A, Sun Y, Li H: Characterization of folate-graft-chitosan as a scaffold for nitric oxide release. *Int J Biol Macromol*, 2008; 43(5): 415-21
- Tu YS, Fu JW, Sun DM et al: Preparation, characterisation and evaluation of curcumin with piperine-loaded cubosome nanoparticles. *J Microencapsul*, 2014; 31(6): 551-59
- Muller F, Salonen A, Glatter O: Phase behavior of Phytantriol/water bicontinuous cubic Pn3m cubosomes stabilized by Laponite disc-like particles. *J Colloid Interface Sci*, 2010; 342(2): 392-98
- Bwatanglang IB, Mohammad F, Yusof NA et al: Folic acid targeted Mn: ZnS quantum dots for theranostic applications of cancer cell imaging and therapy. *Int J Nanomedicine*, 2016; 11: 413-28
- Dabholkar RD, Sawant RM, Mongayt DA et al: Polyethylene glycol-phosphatidylethanolamine conjugate (PEG-PE)-based mixed micelles: Some properties, loading with paclitaxel, and modulation of P-glycoprotein-mediated efflux. *Int J Pharm*, 2006; 315(1-2): 148-57
- Kabanov AV, Batrakova EV, Alakhov VV: Pluronic block copolymers as novel polymer therapeutics for drug and gene delivery. *J Control Rel*, 2002; 82(2-3): 189-212
- Kelemen LE: The role of folate receptor alpha in cancer development, progression and treatment: Cause, consequence or innocent bystander? *Int J Cancer*, 2006; 119(2): 243-50
- Leesajakul W, Nakano M, Taniguchi A, Handa T: Interaction of cubosomes with plasma components resulting in the destabilization of cubosomes in plasma. *Colloids Surf B Biointerfaces*, 2004; 34(4): 253-58
- Bode JC, Kuntsche J, Funari SS, Bunjes H: Interaction of dispersed cubic phases with blood components. *Int J Pharm*, 2013; 448: 87-95

Conflict of interest

None.